80. R. B. Borgens, E. Roederer, M. J. Cohen, *Science* **213**, 611 (1981).
81. A. R. M. Raji and R. E. M. Bowden, *J. Bone Jt. Surg.* **65**, 478 (1983); D. H. Wilson and P. Jagadeesh, *Paraplegia* **14**, 12 (1976).
82. W. M. Cowan, *Int. Rev. Physiol.* **17**, 149 (1978); R. L. Sidman and S. V. O'Gorman, *Adv. Neurol.* **29**, 213 (1981); P. Rakic, *Neurosci. Res. Program Bull.* **20**, 439 (1982).
83. E. A. Heinicke, *Acta Neuropathol.* **49**, 177 (1980); C. C. Kao, *Exp. Neurol.* **44**, 424 (1974); E. L. Weinberg and C. S. Raine, *Brain Res.* **198**, 1 (1980).
84. M. Benfey and A. J. Aguayo, *Nature (London)* **296**, 150 (1982); S. David and A. J. Aguayo, *Science* **214**, 931 (1981); P. M. Richardson, U. M. McGuiness, A. J. Aguayo, *Brain Res.* **237**, 147 (1982).
85. L. F. Kromer, A. Bjorklund, U. Stenevi, *Brain Res.* **210**, 173 (1981).
86. B. H. Hallas, *Experientia* **38**, 699 (1982).
87. H. Nornes, A. Bjorklund, U. Stenevi, *Cell Tissue Res.* **230**, 15 (1983).
88. L.-G. Nygren, L. Olsen, A. Seiger, *Brain Res.* **129**, 227 (1977).
89. U. Patel and J. J. Bernstein, *J. Neurosci. Res.* **9**, 303 (1983); J. J. Bernstein *et al.*, *ibid.* **11**, 359 (1984).
90. R. L. Sidman and N. K. Wessells, *Exp. Neurol.* **48**, 237 (1975).
91. J. C. De La Torre, P. K. Hill, M. Gonzalez-Carvajal, J. C. Parker, Jr., *ibid.* **84**, 188 (1984).
92. J. Silver and M. Y. Ogawa, *Science* **220**, 1067 (1983).
93. W. Schultz, *Prog. Neurobiol.* **18**, 121 (1982); O. Hornykiewicz, *Life Sci.* **15**, 1249 (1974).
94. W. J. Freed *et al.*, *Ann. Neurol.* **8**, 510 (1980); M. J. Perlow *et al.*, *Science* **204**, 643 (1979).
95. A. Bjorklund *et al.*, *Brain Res.* **199**, 307 (1980); A. Bjorklund, R. H. Schmidt, U. Stenevi, *Cell Tissue Res.* **212**, 39 (1980).
96. S. B. Dunnett *et al.*, *Acta Physiol. Scand.* **522**, 29 (1983); S. B. Dunnett *et al.*, *ibid.*, p. 39; F. H. Gage, S. B. Dunnett, U. Stenevi, A. Björklund, *Science* **221**, 966 (1983).
97. W. J. Freed *et al.*, *Science* **222**, 937 (1983).
98. W. J. Freed, *Biol. Psychiatry* **18**, 1205 (1983).
99. S. M. Wuerthele *et al.*, *Exp. Brain Res.* **44**, 1 (1981).
100. S. R. Snyder, D. Sahar, A. L. N. Prasad, S. Fahn, *Life Sci.* **20**, 1077 (1977); R. J. Wurtman, L. A. Pohorecky, B. S. Baliga, *Pharmacol. Rev.* **24**, 411 (1972).
101. W. F. Freed *et al.*, *Brain Res.* **269**, 184 (1983); I. Stromberg *et al.*, *ibid.* **297**, 41 (1984).
102. W. J. Freed *et al.*, *Nature (London)* **292**, 351 (1981).
103. W. J. Freed and H. E. Cannon-Spoor, *Soc. Neurosci. Abstr.* **10**, 666 (1984).
104. J. M. Morihisa *et al.*, *Exp. Neurol.* **84**, 643 (1984).
105. S. C. McLoon and R. D. Lund, *Exp. Brain Res.* **40**, 273 (1980).
106. S. C. McLoon and R. D. Lund, *J. Comp. Neurol.* **217**, 376 (1983).
107. W. J. Freed and R. J. Wyatt, *Life Sci.* **27**, 503 (1980).
108. C. B. Jaeger and R. D. Lund, *Neuroscience* **7**, 3069 (1982); H. Bjorklund *et al.*, *Dev. Brain Res.* **9**, 171 (1983).
109. C. B. Jaeger and R. D. Lund, *J. Comp. Neurol.* **194**, 571 (1980).
110. G. D. Das, B. H. Hallas, K. G. Das, *Am. J. Anat.* **158**, 135 (1980); M. K. Floeter and E. G. Jones, *J. Neurosci.* **4**, 141 (1984).
111. R. Labbe, A. Firl, Jr., E. J. Mufson, D. G. Stein, *Science* **221**, 470 (1983).
112. D. Gash, J. R. Sladek, Jr., C. D. Sladek, *ibid.* **210**, 1367 (1980).
113. D. T. Krieger *et al.*, *Nature (London)* **298**, 468 (1982).
114. G. W. Arendash and R. A. Gorski, *Science* **217**, 1276 (1982).
115. L. F. Kromer, A. Bjorklund, U. Stenevi, *J. Comp. Neurol.* **218**, 433 (1983); E. R. Lewis and C. W. Cotman, *Neuroscience* **8**, 57 (1983).
116. S. B. Dunnett *et al.*, *Brain Res.* **251**, 335 (1982); also compare F. H. Gage *et al.*, *Science* **225**, 533 (1984).
117. J. S. Petrofsky and C. A. Phillips, *J. Neurol. Orthopedic Surg.* **4**, 153 (1983).
118. R. White, *IEEE Trans. Biomed. Eng.* **29**, 233 (1982).
119. W. H. Dobelle, M. G. Mladejovsky, J. P. Girvin, *Science* **183**, 440 (1974).
120. J. Pine, *J. Neurosci. Methods* **2**, 19 (1980).
121. A. M. Turner and W. T. Greenough, *Acta Sterelogica* **2** (Suppl. 1), 239 (1983); A. Basso, E. Capitani, L. A. Vignolo, *Arch. Neurol.* **36**, 190 (1979).
122. Such as activation of dormant genes [M. A. DiBerardino, N. J. Hoffer, L. D. Etkin, *Science* **224**, 946 (1984)].
123. R. W. Sperry, *Proc. Natl. Acad. Sci. U.S.A.* **50**, 703 (1963).

RESEARCH ARTICLE

Three-Dimensional Flow in the Upper Ocean

Robert A. Weller, Jerome P. Dean, John Marra
James F. Price, Erika A. Francis, David C. Boardman

Regularly spaced, long, narrow surface slicks or rows of flotsam are commonly observed on the surface of windswept lakes and seas. In 1927, while on an Atlantic crossing to England, Irving Langmuir (*1*) observed such parallel lines of floating seaweed. After he returned home to New York, Langmuir conducted a series of ingenious flow visualization experiments in Lake George, showing that the slicks are formed in regions of convergent surface flow which are associated with counterrotating helical vortices near the surface of the lake. The rotational axes of the vortices were horizontal and nearly parallel to the direction of the wind. These helical flow patterns are now called Langmuir circulation or, individually, Langmuir cells. Today we know that surface slicks are caused by other processes as well as by Langmuir circulation. However, in the open ocean, under moderate to heavy winds, surface slicks or rows of floating seaweed that are aligned nearly parallel to the wind are taken as evidence that helical Langmuir circulation is present within the mixed layer.

Meteorologists and physical, chemical, and biological oceanographers are interested in Langmuir circulation and in any other organized three-dimensional flows in the upper ocean because such flows should be effective mechanisms for transporting horizontal momentum, heat, nutrients, and organisms vertically through the wind-stirred upper boundary or mixed layer of the ocean. The field measurements collected to date, however, are insufficient to describe the persistence, depth of penetration, and amplitude of the helical flow. Thus, only limited evidence for such vertical transport exists.

Woodcock (*2*), for example, observed that buoyant *Sargassum* was carried under the surface in the regions of convergent surface flow. Accordingly, phytoplankton, with small terminal velocities (*3*), should be carried along with the helical flow and experience large changes in irradiance (*4*), affecting their photosynthesis (*5–7*); yet that conclusion is presently based almost entirely on laboratory experiment (*5, 8*) and theoretical inference (*9–11*). Recently, in Loch Ness, Thorpe and Hall (*12*) observed tongues of warm water extending downward toward the base of the mixed layer from beneath surface slicks. Such evidence from field studies (*13, 14*), recent laboratory experiments (*15*), and numerical models (*16*) suggest, but do not prove, that three-dimensional flow such as Langmuir circulation plays an important role in upper ocean processes.

Recently we began a study of the physics and biology of the mixed layer, including an investigation of the role of organized, three-dimensional flows. Our first goal was to develop the capability to make accurate measurements in the upper ocean of the vertical and horizontal components of velocity, the temperature, the conductivity, and the concentrations of chlorophyll a (a good indica-

Robert Weller, Jerome Dean, James Price, and Erika Francis are members of the research staff at the Woods Hole Oceanographic Institution, Woods Hole, Massachusetts 02543. John Marra and David Boardman are members of the research staff at the Lamont-Doherty Geological Observatory, Palisades, New York 10964.

tor of phytoplankton biomass). The chlorophyll a content would serve both as additional data for evaluating mixed layer dynamics and as a means to study the effect of the three-dimensional flow on biological processes in the upper ocean. Our second goal was to observe and characterize the vertical and horizontal velocities, temperature, conductivity fluctuations, and the chlorophyll a concentration associated with Langmuir circulation.

Instruments and methods. Previous measurements suggested that the fluctuations we hoped to measure would be small relative to other variability in the mixed layer. Near-surface vertical velocities associated with Langmuir circulation had been reported to increase with wind speed at approximately 0.0085 m sec^{-1} of near-surface downwelling velocity per 1 m sec^{-1} of wind (*13, 14*). In comparison, the vertical velocities associated with surface gravity waves are an order of magnitude larger. Thorpe and Hall (*12*) found the downwelling fluid beneath slick lines to be approximately 0.0002°C warmer than other fluid at the same depth; diurnal temperature changes in the mixed layer can exceed 0.5°C. Unwanted motion of the instruments themselves would complicate the task of measuring such small changes. Temperature, conductivity, and chlorophyll a content have large vertical gradients at some depths in the upper ocean; and instruments lowered from a rolling ship would, due to their vertical motion, measure at those depths large fluctuations in temperature, conductivity, and chlorophyll a content in addition to fluctuations in vertical velocity. Because of the low signal-to-noise ratios it was necessary to develop a new instrument for making direct measurements of vertical velocities in the mixed layer and to deploy all the instrumentation from a platform that did not roll and heave in response to surface waves.

The new instrument, called the real-time profiler (RTP), directly measures vertical velocities as well as horizontal velocities, temperature, and conductivity. Another instrument, used for horizontal velocity measurements in the upper ocean and called the vector-measuring current meter (VMCM), had previously been developed and found to make accurate measurements of low-amplitude, low-frequency horizontal flows in the presence of surface waves (*17, 18*). The velocity sensor of the VMCM consists of two cosine-response propeller assemblies mounted at right angles. For our purpose, two such sensors were mounted at right angles on the RTP with the axis of rotation of one propeller assembly on each sensor oriented vertically (Fig. 1). A fin attached to the pressure case that housed the electronics oriented the instrument with respect to the mean flow so that the velocity sensors were upstream of the pressure housing. The two vertically oriented propeller assemblies produced redundant vertical velocity measurements. The two horizontally oriented propeller assemblies measured orthogonal components of velocity, which, together with the heading from a compass in the instrument, were later transformed into the east and north components of horizontal velocity. In addition, the instrument was fitted with an external temperature sensor, a conductivity sensor, a pressure sensor, and two accelerometers that sensed tilt. Information from the accelerometers was transmitted as an analog signal up an electromechanical cable. All other data from the RTP were both recorded internally and transmitted in digital format up the cable every 14 seconds. The least counts in the digitization of temperature (0.005°C), pressure (0.16 dbar), and conductivity (0.0025 mS cm^{-1}) were well within the precision of the sensors and associated circuitry. A fluid velocity of 0.01 m sec^{-1} was required before the propellers would record it. One count from the velocity sensors corresponded to a displacement of approximately 0.08 m of fluid parallel to the propeller's axis of rotation.

Abstract. *Measurements made from the Research Platform* FLIP *provide some of the first direct observations of three-dimensional flow within the surface mixed layer of the ocean. Relatively narrow regions of downwelling flow were found within the mixed layer, in coincidence with bands of convergent surface flow. At mid-depth in the mixed layer, the downwelling flow had magnitudes of up to 0.2 meter per second and was accompanied by a downwind, horizontal jet of comparable magnitude. There is some evidence that these motions transport heat and phytoplankton within the mixed layer.*

In order to take chlorophyll a measurements, a fluorometer package was deployed with the RTP. The fluorometer package consisted of a SeaMarTec in situ fluorometer, temperature and pressure sensors, and a Sea Data data logger. It was calibrated by taking samples of water in Niskin bottles at the same time and depth as the fluorometer readings, and filtering the water samples for later chlorophyll a analysis by fluorometry. The fluorometer package was shackled directly below a VMCM, which was in turn shackled directly below the RTP; the VMCM provided an independent record of temperature, horizontal velocity, and pressure.

Our first deployment of these instruments was made from the Research Plat-

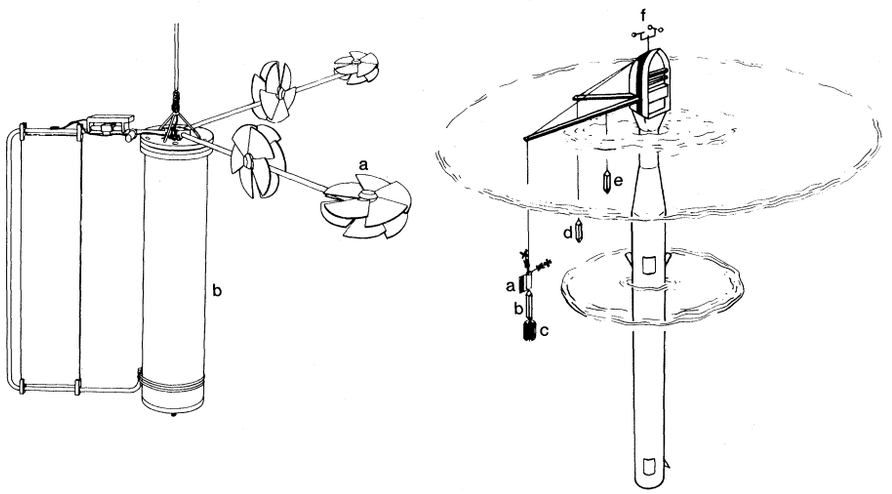

Fig. 1 (left). The real-time profiler was used to measure vertical and horizontal velocities, temperature, conductivity, and pressure. The electronics package also measured the orientation and tilt of the instrument. The propeller sensors (a) were 0.22 m in diameter; the pressure case that housed the electronics (b) was 1.22 m in length and 0.19 m in diameter. Fig. 2 (right). The Research Platform *FLIP* as rigged in December 1982. The instruments were: (a) the real-time profiler, (b) a vector-measuring current meter (VMCM), (c) the SeaMarTec fluorometer and data logger, (d) a profiling VMCM, (e) a VMCM held at a depth of 2 m, and (f) meteorological sensors.

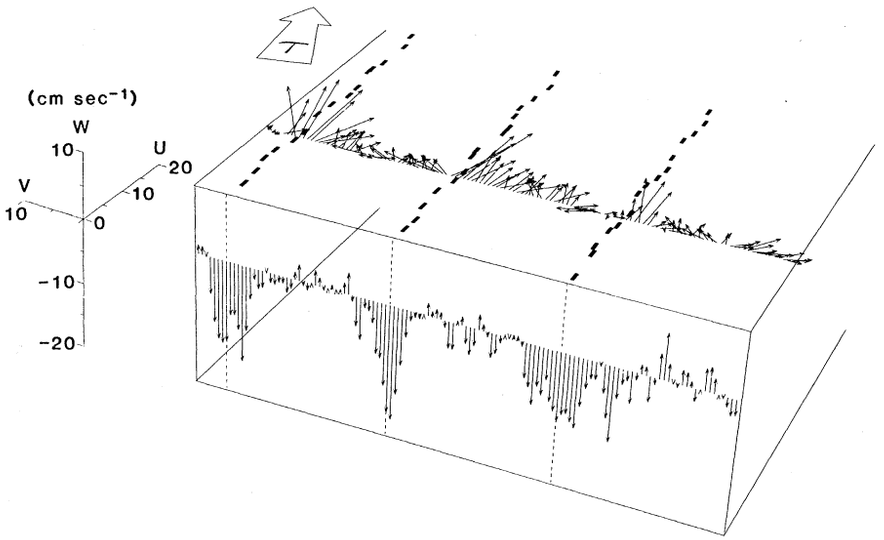

Fig. 3. This is a three-dimensional presentation of the time series taken by the RTP between 10:30 and 11:00 a.m. local time, 13 December 1982. U, V, and W are the east-west, north-south, and vertical components of the fluid velocity, respectively. The irregularly positioned rectangles in three lines on the surface were drawn in to simulate the long, narrow bands of computer cards that were observed on the sea surface at this time. The vertical arrows are individual values, drawn every 14 seconds on a time axis that runs from left to right, of vertical velocity at 23 m. The horizontal arrows (drawn on the top surface for clarity) are the horizontal velocities observed at 23 m. The broad arrow labeled τ shows the direction of the wind at the time. The vertical velocity data have been corrected for tilt of the RTP; the correction was of order 0.01 m sec^{-1}. A three-point running mean was applied to both the horizontal and vertical velocities before drawing this figure.

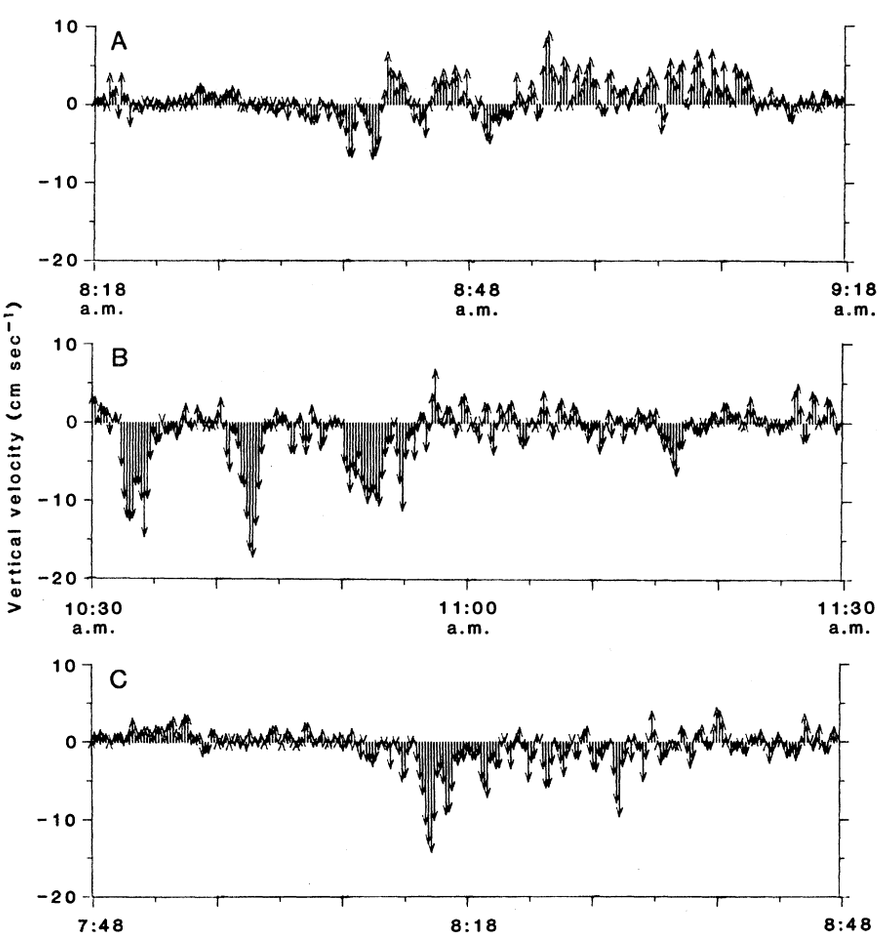

Fig. 4. Three time series of vertical velocity from 13 December. As in Fig. 3, a three-point running mean was applied to the time series. This removes fluctuations in the vertical velocity associated with wave motion; untreated data are shown in Fig. 5.

form *FLIP*. The *FLIP* was towed to the site of the experiment in the horizontal position; and once at the site, tanks in the hull were flooded to pivot the *FLIP* upright. In the upright working position, with 95 m of hull below the waterline, the *FLIP* is stable compared to ships or shallow draft surface buoys (*19*). As a result, instrumentation lowered from the *FLIP* does not move up and down as it would if lowered from a rolling ship. Booms were rigged from the *FLIP* so that the suspended instruments were kept away from the hull (Fig. 2), and a thruster (on the hull but not aimed at or near the instruments) maintained the vessel's orientation so that the instruments were not in the *FLIP*'s wake as it slowly drifted through the ocean.

From 12 to 16 December 1982 measurements were made as the *FLIP* drifted southward off the coast of southern California southwest of San Clemente Island. Surface wave heights and wind speeds were moderate, averaging approximately 1 m and 8 m sec^{-1}, respectively, with the highest winds (14 m sec^{-1}) occurring on the morning of the 13th. The seasonal thermocline began at an average depth of 50 m. The horizontal velocity field relative to the *FLIP* had magnitudes of approximately 0.1 m sec^{-1}. The RTP was sometimes positioned at different fixed depths in order to record time series of velocity, temperature, conductivity, and chlorophyll a concentration. At other times the instruments were moved slowly up and down in order to measure vertical profiles. Correcting the measured vertical velocities for the motion of the package was done by converting the rate of vertical displacement of the RTP determined from the pressure sensor to vertical velocity and subtracting that from the measured vertical velocity.

Observations of three-dimensional flow. One set of velocity time series, measured at a depth of 23 m, will be discussed in detail as an example of the observations collected by these methods. The rest of the data, both the remaining time series taken at fixed depths and the vertical profiles, will be discussed more concisely and used to develop a list of the characteristics of the three-dimensional flow that was observed during this experiment.

At about 10:30 a.m. (local time) on 13 December the three instruments were fixed with the RTP at a depth of 23 m, roughly at mid-depth in the mixed layer. The data taken by the RTP over the next 30 minutes are represented in Fig. 3, and the sequence of events that began at 10:30 a.m. can be summarized as follows: Soon after 10:30 a.m. downwelling

velocities as high as -0.18 m sec^{-1} were observed. At that time, used computer cards were scattered from various locations on the *FLIP* to cover the sea surface; within 1 to 2 minutes these cards were drawn into long, narrow bands approximately 20 m apart. The lines of cards formed at an angle of approximately 15° to the right of the wind. The cable to which the RTP was attached cut through one of these lines of cards at 10:42 a.m. and again at 10:52 a.m. Persistent downward flow was observed by the RTP for a period of approximately 2 minutes beginning shortly after 10:40 a.m. and again shortly after 10:50 a.m., bracketing the times at which the cable passed through the card lines. The horizontal velocities observed by both the RTP and VMCM turned downwind and intensified markedly when the downwelling was encountered. The downwind horizontal jets reached the same magnitude, approximately 0.2 m sec^{-1}, as the downwelling velocity. The flow beneath the card lines was thus, at 23 m, directed downward at an angle of close to 45° and was nearly three times as strong as the typical downward flow in the mixed layer during this experiment. The three instruments were kept at the same depth for another 70 minutes following 11:00 a.m., but in that period the downwelling events were both weaker and less concentrated.

To help place the measurements taken from 10:30 to 11:00 a.m. in context, Fig. 4 shows three time series of vertical velocity measured at different times on 13 December; Fig. 4B includes the 30 minutes of data used in Fig. 3. From 8:18 to 9:18 a.m. downwelling and upwelling flows, both with magnitudes of up to 0.07 m sec^{-1}, were observed at a depth of 9.5 m. The horizontal flow did not turn toward the downwind direction during this hour. From 10:30 to 11:00 a.m. the three strong downwelling events discussed above were observed at 23 m; in the next 30 minutes only one downwelling event, with a maximum speed of 0.08 m sec^{-1}, was observed. From 7:48 to 8:48 p.m., at 21 m, a single strong downwelling jet was observed in coincidence with a downwind jet of the same strength.

Downwelling flows similar to those seen on 13 December, with magnitudes of 0.10, 0.17, and 0.20 m sec^{-1}, were observed on the morning of 15 December, when the wind speed was 2.3 m sec^{-1}, on that afternoon, when the wind speed was 2.6 m sec^{-1}, and at midday on 16 December, when the wind speed was 6.6 m sec^{-1}, respectively. Aerial photographs of surface slicks (*20, 21*) had led us to expect regularly spaced Langmuir cells that extended, one after the other, over large areas of the ocean. However, the strongest three-dimensional flows, such as shown in Fig. 3, were only intermittent. More typical were downwelling flows between 0.05 and 0.10 m sec^{-1}, with no obvious associated change in the horizontal velocity.

Downwelling flows were observed only when surface drifters scattered from the *FLIP* aligned relatively quickly. During the day computer cards were used as surface drifters, as discussed above. During the night small, flat plastic bags partially filled with luminescent fluid were used in place of the computer cards. The strength of the observed downwelling varied with the rate of alignment of these drifters, indicating that the strength of the interior flow varied with the strength of the surface flow. When the drifters failed to align or aligned slowly, taking 15 minutes or longer, the vertical velocities measured by the RTP changed sign frequently and had mean values of approximately 0.02 m sec^{-1}.

The dependence of the downwelling velocity on wind speed suggested in the literature (*13, 14*) was not verified by this data. The downwelling velocities were, however, strongly depth dependent. The strongest downwelling flows were observed at depths between 10 and 35 m, corresponding to the middle region of the mixed layer; above and below that region downwelling flows, if observed, were typically less than 0.05 m sec^{-1}. No evidence of downwelling flow was found in or below the seasonal thermocline.

We believe the three-dimensional velocity structures described above to be genuine features of the upper ocean flow field. However, several possible error sources merit brief discussion. Tilting the RTP in the presence of a horizontal current will cause a vertical velocity to be measured. Measured tilts of the RTP were small, within 3° of vertical, so that the component of the mean horizontal velocity field sensed by the vertically oriented propellers was less than 5 percent of the horizontal velocity. Between 10:30 a.m. and 12:10 p.m. on 13 December, this would be 0.01 m sec^{-1}, small compared to the measured downwelling.

When held at a fixed depth the RTP was pulled up and down by the *FLIP*'s small roll and heave. The observed dis-

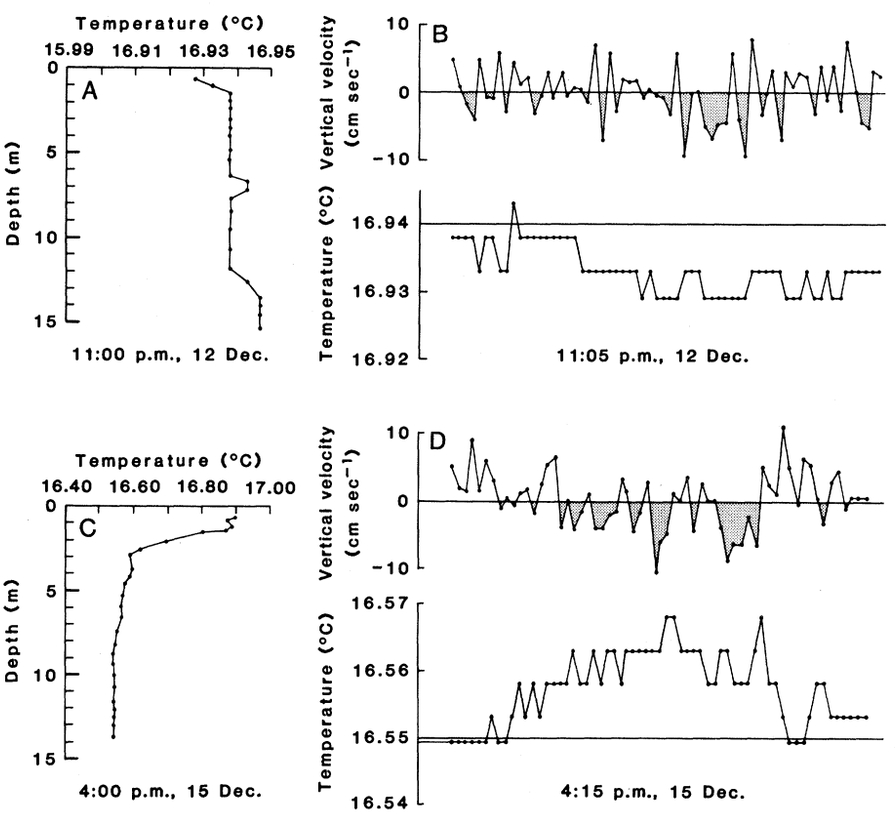

Fig. 5. (A) At 11:00 p.m. local time on 12 December a vertical temperature profile showed that the near-surface region was slightly cooler than the interior of the surface layer. (B) Unaveraged time series of vertical velocity and temperature showed that negative temperature anomalies were encountered in regions of downward flow; the time series show approximately 15 minutes of the original data collected at mid-depth in the mixed layer. (C) At 4:00 p.m. local time on 15 December a vertical profile of temperature showed that the near-surface region was slightly warmer than the interior. (D) The 15-minute, unaveraged time series showed that slightly warmer temperatures were encountered in downwelling regions by the RTP.

placement of the RTP was at most a 0.30 m amplitude oscillation with a period of approximately 120 seconds. Long-term averages of vertical velocity were computed for various depths below the mixed layer to verify that the velocity sensors properly measured the fluctuation in the flow; the magnitudes of such averages were between 0.001 and 0.0001 m sec^{-1}.

Near the surface, surface wave velocities were also present. In the absence of the downwelling events discussed in the previous section, 30-minute average vertical velocities computed from data taken in the mixed layer were between 0.01 and 0.001 m sec^{-1} in magnitude. These mean vertical velocities were small enough to show that neither surface wave velocities nor motion of the instrument induced false vertical velocity signals as large as those observed, which had magnitudes as high as 0.22 m sec^{-1} and, typically, were between 0.05 and 0.10 m sec^{-1}. However, averaging across individual events such as those shown in Fig. 3 did not always yield near-zero vertical velocities, as might be anticipated. The data are time series taken from a drifting platform. Thus, it is possible that the *FLIP* spent more time in the convergent, downwelling regions than in the regions of weak upwelling and that nonzero averages of vertical velocity do not imply either a lack of continuity or an error in the measurements.

Further, periods with persistent downwelling velocities greater than 0.04 m sec^{-1} were observed by the RTP only when the surface drifters also formed into lines nearly parallel to the wind. Under a variety of wind and wave conditions, whenever the drifters failed to align or aligned only after relatively long times, there was no indication of a persistent vertical flow in the upper ocean. If large vertical velocities could be introduced into the RTP measurements by surface wave or platform motion, then large vertical flows should have been indicated throughout the entire experiment, not just when patterns of convergent surface flow were present.

Consequences of organized three-dimensional flow in the mixed layer. During the day incoming solar radiation heats the upper ocean, but the amount of radiation that penetrates the ocean decays exponentially. As a result, a shallow, warm layer may tend to form at the surface during midday. At night the surface of the ocean loses heat to the atmosphere and fluid at the surface may be cooler than that in the interior. The convergent surface flow visualized by the surface drifters should concentrate the warmed or cooled surface water in the area of downwelling where it would be carried downward into the interior of the mixed layer, as seen in Loch Ness (*12*). The temperature data from the RTP were examined for evidence that the observed three-dimensional flow transported heat through the mixed layer. Temperature anomalies were found in the downwelling regions. Positive anomalies were observed during midday and negative anomalies were observed during the night, when near-surface temperatures were warmer and cooler, respectively, than the interior of the mixed layer (Fig. 5). The observed temperature anomalies were ≤ 0.015°C, which is consistent with a surface transit time of a few minutes and a surface heat flux on the order of 500 W m^{-2}.

Often the mixed layer was well mixed with respect to chlorophyll a, and chlorophyll concentrations in the downwelling flows were not significantly different from concentrations elsewhere in the mixed layer. When vertical profiles of chlorophyll in the mixed layer were not uniform, anomalies of up to 0.8 μg per liter were found in association with the downwelling regions, evidence that the downwelling flow carried phytoplankton with it.

Anomalies of temperature and chlorophyll content found in the downwelling regions show that the observed three-dimensional flow carries fluid from the surface down into the interior of the mixed layer. The magnitude of the observed vertical flow is large compared to the terminal velocities of phytoplankton (*3*) and fish eggs (*22*). Hence, Langmuir circulations should play an important role in the biology as well as in the physics of the mixed layer.

References and Notes

1. I. Langmuir, *Science* **87**, 119 (1938).
2. A. H. Woodcock, *J. Mar. Res.* **9** (No. 2), 77 (1950).
3. T. J. Smayda, *Oceanogr. Mar. Biol.* **8**, 353 (1970).
4. K. L. Denman and A. E. Gargett, *Limnol. Oceanogr.* **28**, 801 (1983).
5. J. Marra, *Mar. Biol.* **46**, 191 (1978).
6. G. P. Harris and J. N. A. Lott, *J. Fish. Res. Board Can.* **30**, 1771 (1973).
7. J. Marra, *Mar. Biol.* **46**, 203 (1978).
8. R. H. Stavn, *Limnol. Oceanogr.* **16**, 453 (1971).
9. H. Stommel, *J. Mar. Res.* **8**, 24 (1949).
10. M. Ledbetter, *Ecol. Model.* **7**, 289 (1979).
11. G. T. Evans and F. J. R. Taylor, *Limnol. Oceanogr.* **25**, 840 (1980).
12. S. A. Thorpe and A. J. Hall, *J. Fluid Mech.* **114**, 237 (1982).
13. R. T. Pollard, in *A Voyage of Discovery, George Deacon 70th Anniversary Volume*, M. V. Angel, Ed. (Pergamon, New York, 1977), p. 235.
14. S. Leibovich, *Annu. Rev. Fluid Mech.* **15**, 391 (1983).
15. A. J. Faller, *Science* **201**, 618 (1978).
16. A. D. P. Craik and S. Leibovich, *J. Fluid Mech.* **73**, 401 (1976).
17. R. E. Davis and R. A. Weller, in *Air-Sea Interaction: Instruments and Methods*, F. Dobson, L. Hasse, R. Davis, Eds. (Plenum, New York, 1980), p. 481.
18. R. A. Weller and R. E. Davis, *Deep-Sea Res.* **27A**, 565 (1980).
19. P. Rudnick, *J. Ship Res.* **11**, 257 (1967).
20. H. Stommel, *Weather* **6**, 72 (1951).
21. A. J. Faller, *Tellus* **16**, 365 (1964).
22. S. Sundby, *Deep-Sea Res.* **30**, 645 (1983).

23. This work was supported by the Office of Naval Research through contracts N0014-76-C-0197 and NR083-400 to Woods Hole Oceanographic Institution and contract N0014-80-C0098-II to Lamont-Doherty Geological Observatory of Columbia University. This manuscript is Contribution 5439 from Woods Hole Oceanographic Institution. Discussions or correspondence with A. Faller, H. Stommel, J. Steele, K. Brink, and others during the preparation of this manuscript are gratefully acknowledged.

21 December 1983; accepted 23 July 1984